JOURNAL OF GEOPHYSICAL RESEARCH, VOL. 114, D00F08, doi:10.1029/2008JD011688, 2009

Relationship between photochemical ozone production and NO_x oxidation in Houston, Texas

J. A. Neuman,[1,2] J. B. Nowak,[1,2] W. Zheng,[3] F. Flocke,[3] T. B. Ryerson,[2] M. Trainer,[2] J. S. Holloway,[1,2] D. D. Parrish,[2] G. J. Frost,[1,2] J. Peischl,[1,2] E. L. Atlas,[4] R. Bahreini,[1,2] A. G. Wollny,[1,2] and F. C. Fehsenfeld[1,2]

Received 31 December 2008; revised 17 March 2009; accepted 23 March 2009; published 23 May 2009.

[1] An instrumented aircraft was used to study anthropogenic emissions and subsequent ozone and reactive nitrogen photochemistry in the continental boundary layer downwind of Houston, Texas. Measurements of ozone, carbon monoxide, NO_x, and NO_x oxidation products were conducted from the NOAA WP-3 aircraft during the 2006 Texas Air Quality Study under a variety of meteorological conditions. Sixty-five crosswind transects of plumes from Houston urban and industrial areas performed on 10 daytime flights from 13 September to 6 October 2006 are examined. Coincident measurements of NO_x and its oxidation products show that NO_x was oxidized predominately to nitric acid and peroxy acyl nitrates on time scales of a few hours. The observed relationships between O_3 and NO_x oxidation products are affected by both photochemistry and mixing of different air masses. On four flights, background pollutant mixing ratios were constant and CO to NO_y enhancement ratios in downwind plume transects remained at the emission ratio. The enhancement ratio of O_3 to NO_x oxidation products was also nearly constant and could be used to derive ozone production efficiency (OPE) in plumes downwind from the Houston area. On the other flights, variable mixing of regionally polluted background air with plumes caused CO to NO_y and O_3 to $NO_y - NO_x$ enhancement ratios to increase as plumes were transported. In such cases, enhancement ratios do not solely reflect plume processing, and OPE could not be determined. The OPE averages 5.9 ± 1.2 in coalesced plumes from urban and petrochemical industrial sources in Houston, with higher values in isolated plumes downwind from petrochemical facilities located along the Houston ship channel.

Citation: Neuman, J. A., et al. (2009), Relationship between photochemical ozone production and NO_x oxidation in Houston, Texas, *J. Geophys. Res.*, *114*, D00F08, doi:10.1029/2008JD011688.

1. Introduction

[2] NO_x(=NO + NO_2) abundance affects ozone (O_3) formation [*Liu et al.*, 1987], and the relationship between O_3 and its NO_x precursors has been examined for over 20 years. Understanding the dependence of O_3 upon NO_x and the fate of NO_x and its oxidation products is necessary to accurately determine the factors that control O_3 pollution. The number of O_3 molecules formed for each NO_x molecule emitted or oxidized is often called the ozone production efficiency (OPE), and it is valuable for assessing the photochemistry responsible for O_3 production [*Trainer et al.*, 1993]. Effective O_3 control strategies based on NO_x emission reductions must account for variations in OPE, which depend upon location, NO_x source strength [*Ryerson et al.*, 2001], and coemission of volatile organic compounds (VOC) that are O_3 precursors [*Ryerson et al.*, 2003].

[3] O_3 is often highly correlated with the products of NO_x oxidation [*Trainer et al.*, 1993], whereupon an observationally based estimate of OPE can be directly obtained from the observed ratio of O_3 to the products of NO_x oxidation. This estimate represents the net O_3 production and NO_x oxidation in a sampled air mass integrated over the time from emission until measurement. However, NO_x oxidation products and O_3 can be removed from the atmosphere at different rates so that their relationship also reflects physical removal processes and is not solely determined by photochemistry [*Trainer et al.*, 1993, 2000]. Nitric acid (HNO_3), which is often the most abundant product of NO_x oxidation, can be rapidly removed from the atmosphere by dry and wet deposition [*Hanson and Lindberg*, 1991; *Munger et al.*, 1998; *Neuman et al.*, 2004]. When NO_x oxidation products are lost from the atmosphere more rapidly than O_3, the observed ratio of O_3 to NO_x oxidation products overestimates the number of O_3 molecules produced from each NO_x

[1]Cooperative Institute for Research in Environmental Sciences, University of Colorado at Boulder, Boulder, Colorado, USA.
[2]Earth System Research Laboratory, NOAA, Boulder, Colorado, USA.
[3]Atmospheric Chemistry Division, National Center for Atmospheric Research, Boulder, Colorado, USA.
[4]Rosenstiel School of Marine and Atmospheric Sciences, University of Miami, Miami, Florida, USA.

0148-0227/09/2008JD011688$09.00

molecule oxidized [*Trainer et al.*, 1993; *Sillman et al.*, 1998]. Thus, determinations of OPE from observed ratios of O_3 to NO_x oxidation products have been qualified with the caveat that any significant removal of NO_x oxidation products from the atmosphere would increase the ratio and give inaccurate results [*Trainer et al.*, 1993, 2000]. For sources that coemit CO and NO_x, such as urban areas, OPE also can be determined from the measured ratio of O_3 to carbon monoxide (CO) and the inventoried or measured CO to NO_x emission ratios. This determination is independent of HNO_3 removal. OPE determined from the ratio of O_3 to NO_x oxidation products can be 2 to 5 times higher than OPE determined using O_3 to CO ratios [*Hirsch et al.*, 1996; *Trainer et al.*, 2000], suggesting that bias from differential removal was substantial.

[4] Large emissions of NO_x from power plants and VOC and NO_x from mobile sources and petrochemical industrial facilities in the Houston area produce some of the highest O_3 mixing ratios observed in the United States (http://www.epa.gov/air/airtrends/2008). Consequently, this region has been studied extensively with the goal of developing effective O_3 mitigation strategies. Measurements from aircraft and ground sites during the Texas 2000 Air Quality Study showed that O_3 formation rates and efficiencies were very high in plumes from petrochemical industrial sources in this region [*Ryerson et al.*, 2003; *Daum et al.*, 2003; *Berkowitz et al.*, 2004; *Kleinman et al.*, 2005]. The rates and pathways of NO_x oxidation were also examined during the Texas 2000 study, showing differences in reactive nitrogen processing in isolated plumes from different anthropogenic source types [*Neuman et al.*, 2002] and high HNO_3 loss rates in power plant plumes [*Neuman et al.*, 2004]. This same region is reexamined here, using data from the 2006 Texas Air Quality Study, and includes analyses of coalesced urban and petrochemical plumes.

[5] In this work, the relationship between O_3 and NO_x oxidation products is studied in plumes from the same source region under a variety of meteorological conditions. In many studies of photochemistry in urban or industrial plumes, direct estimations of OPE from observations implicitly assume that the emissions are released from a localized source into a uniform background and are transported downwind under constant wind speed and direction. As a consequence, the reported results may not be representative of more complex conditions influenced by emissions from multiple sources and variations in wind speed and direction that complicate mixing during transport. This study examines the relationship between O_3 and NO_x oxidation products for all available data to reveal the conditions responsible for a wide range of observed relationships between O_3 and NO_x oxidation products. Determinations of OPE that accurately represent the number of O_3 molecules formed for each NO_x molecule oxidized are achieved by accounting for the influence of changing backgrounds on the measured mixing ratios.

2. Experiment

2.1. Sampling Platform

[6] Between 11 September and 12 October 2006, the NOAA WP-3 aircraft conducted 16 research flights from Ellington Field, Texas, as part of the 2006 Texas Air Quality Study. The present analysis uses data from the 10 daytime flights between 13 September and 6 October 2006 that included multiple crosswind transects of pollution plumes from the Houston area. These 10 flights, with an average duration of 6.2 h, were conducted in the afternoon in order to sample plumes emitted into a well-mixed boundary layer and to best capture photochemical transformations. Flight altitude for the Houston plume studies was usually 500 m above sea level (ASL), and only a few plume transects were performed at higher altitudes within the mixed layer. Altitude profiles were regularly performed outside of plumes, and the maximum altitude on each flight was 3–5.7 km. On each of the Houston flights, several upwind transects and between 4 and 11 downwind plume transects were performed by flying perpendicular to the wind at distances progressively farther downwind from the source region. Consecutive transects were 20–30 km apart, and plumes were sampled up to 170 km from the Houston area. Plumes sampled at the farthest downwind transects had been transported approximately 5 h from the time of emission on most flights.

[7] The analyzed data were obtained from instruments that were similar to those used in a previous experiment conducted aboard the same aircraft [*Neuman et al.*, 2006, and references therein]. Fast response (typically 1 Hz) measurements of nitric oxide (NO), nitrogen dioxide (NO_2), the sum of reactive nitrogen compounds ($NO_y = NO + NO_2 + HNO_3 + PANs + \ldots$), HNO_3, peroxy acyl nitrates (PANs), CO, and O_3 are analyzed, and the measurement details are shown in Table 1. At aircraft flight speeds of 100 m/s, 1-Hz data correspond to measurements averaged over 100 m for each of these species.

2.2. Meteorology

[8] Accounting for variations in background pollutant levels, which contributed to the trace gas mixing ratios measured in plumes downwind from Houston, is necessary to isolate the influence of the urban region. Downtown Houston is 40 km WNW inland from Galveston Bay, which connects to the Gulf of Mexico. When air masses came from the Gulf (south or SE winds) and the air had not been recirculated recently from the continent, background pollutant levels were low with O_3 often less than 20 ppbv, CO approximately 70 ppbv, and NO_y less than 0.4 ppbv. Air masses from the continent (north and NE winds) or recirculated continental air over the Gulf contained higher background levels of pollutants, with O_3 typically 50 ppbv, CO approximately 150 ppbv, and NO_y 1.5–3 ppbv. Since the background levels depend on air mass history and wind direction, meteorology has a strong influence on O_3 mixing ratios in the Houston area. Flights were conducted when winds were from the north, NE, east, SE, and south, so that the study includes plumes superimposed on both continental and marine background air. In contrast to the 2000 study, no flights in 2006 were conducted when winds were from a westerly direction, which has been associated with the development of land-sea breezes that recirculate pollutants [*Darby*, 2005].

[9] During the flights studied here, ambient conditions were typical for summer and fall continental midlatitude locations, with temperatures in the boundary layer of 25°C ± 4°C and relative humidities of 50% ± 20%. The depth of

Table 1. Measurement Techniques for Trace Gas Mixing Ratios

Species	Technique	Inaccuracy	Imprecision	Time Resolution
NO	Chemiluminescence detector (CLD)	±5%	±0.015 ppbv	1 s
NO_2	photolysis converter with CLD	±9%	±0.04 ppbv	1 s
NO_y	300°C gold converter with CLD	±12%	±<0.3 ppbv	1 s
HNO_3	Chemical Ionization Mass Spectrometer (CIMS)	±(15% + 0.1) ppbv	±0.02 ppbv	1 s
PAN, PPN, PiBN	CIMS	±30%		2 s
CO	Vacuum UV fluorescence	±5%	±1 ppbv	1 s
O_3	CLD	±3%	±0.05 ppbv	1 s
SO_2	pulsed UV fluorescence	±10%	±0.3 ppbv	1 s
NO_3^-	C-ToF-AMS	±30%		10–15 s

the boundary layer was usually between 1 and 2 km ASL inland and downwind from Houston, although it was sometimes only a few hundred meters early in the afternoon over Houston. Clouds were rarely encountered, though fair weather cumulus clouds occasionally formed at the top of the boundary layer.

3. Observations

[10] Data from crosswind flight tracks in the Houston vicinity below 1 km altitude are analyzed here. Aircraft flight tracks for two of the ten flights are shown on a map of the region in Figure 1. The center of the Houston urban area is located where many roads (gray lines) converge at 29.8°N, 95.4°W, and the outer beltway around Houston has a 40 km diameter. The Gulf of Mexico is at the lower right-hand corner of Figure 1. The Houston metropolitan area has a population over 5.5 million (www.houstontx.gov/abouthouston/houstonfacts.html). Many petrochemical industrial facilities are located along the Houston ship channel that extends east from the urban area to Galveston Bay.

[11] A time series of 1-s measurements on 25 September 2006 in five crosswind plume transects is shown in Figures 2a and 2b. Since Houston emissions are spread over 40 km in a single direction, the transported plumes were wide (approximately 50 km full width at half maximum). Thus, the duration of each plume crossing was approximately 8 min for the WP-3 aircraft traveling at 100 m/s. The large geographical extent of emissions means that downwind plume transects sampled emissions that were transported over a range of times (typically ±1 h). All the analysis that follows is based on plume transect data from the 15 and 25 September flights shown in Figure 1 and from flights on 13, 19, 20, 21, 26, and 27 September and 5 and 6 October 2006.

3.1. Ozone

[12] Although the measurements reported here occurred after the peak O_3 season, rapid NO_x oxidation and O_3 production were observed on all 10 of the daytime flights in the Houston area. Maximum 1-s O_3 mixing ratios observed from the aircraft exceeded 110 ppbv on half of the flights near Houston and ranged from 72 to 147 ppbv on each flight. On every flight, O_3 mixing ratios in the Houston pollution plume reached levels at least 30 ppbv greater than the upwind background that ranged from 20 to 60 ppbv. Enhancements in O_3 mixing ratios in plumes increased markedly in the first few downwind transects, when NO_x oxidation was large. After most of the NO_x had been oxidized, O_3 mixing ratios remained nearly constant in plume transects farther downwind (e.g., Figure 2), reflecting an approximate balance between production versus dilution

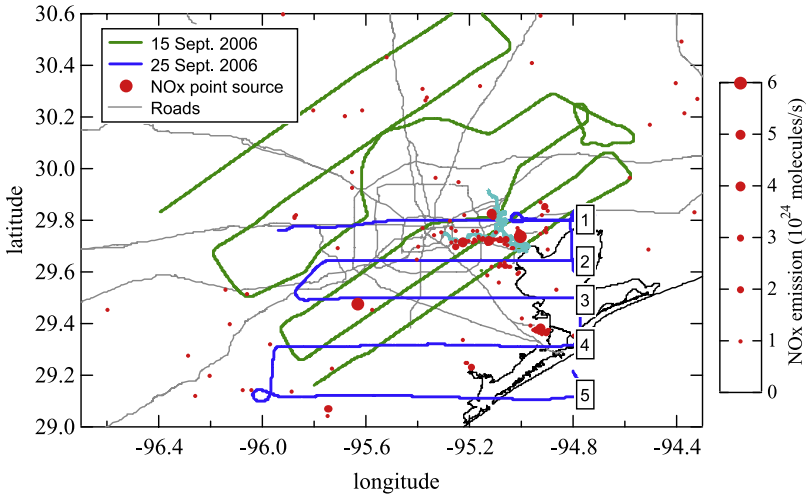

Figure 1. Aircraft flight tracks downwind of Houston urban and industrial areas on 15 (green lines) and 25 September 2006 (blue lines) overlaid on a map of the Houston area. Roads are shown as gray lines, and the Houston ship channel is shown in light blue. The red points are NO_x point sources from the 2004 TCEQ Annual Point Source Emission Inventory with electric power generation facilities updated to 2006 levels, sized according to their emission rates between 10^{22} and 6.3×10^{24} molecules/s. The 25 September transects are labeled according to the order in which they were sampled.

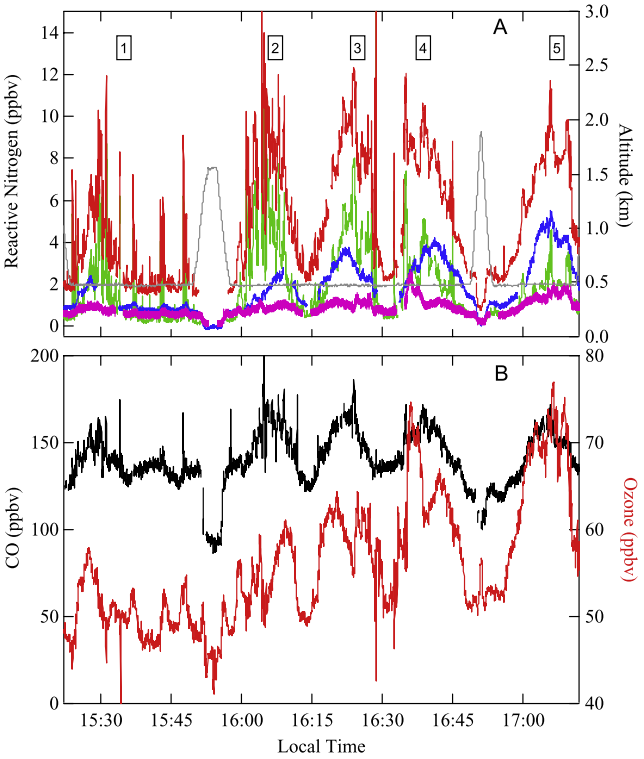

Figure 2. (a) NO_y (red), NO_x (green), HNO_3 (blue), and PANs (pink) mixing ratios measured once per second during plume transects on 25 September 2006. Aircraft altitude is shown in gray (right axis). The numbers correspond to the labels shown in Figure 1. (b) CO (black) and O_3 (red) mixing ratios.

and loss processes, or negligible influence from these effects.

3.2. Reactive Nitrogen Budget

[13] Measurement accuracy and atmospheric composition are examined by comparing the individually measured reactive nitrogen compounds to a measurement of the sum of reactive nitrogen species (NO_y). The sum of the individually measured HNO_3, NO, NO_2, PAN (peroxyacetic nitric anhydride), PPN (peroxypropionic nitric anhydride), and PiBN (peroxyisobutyric nitric anhydride) on 10 daytime flights conducted in the Houston and Dallas areas is compared to the independently measured NO_y in Figure 3. Measurements of compounds that were a small fraction of NO_y on these daytime flights (for example MPAN, APAN, NO_3 and N_2O_5) or that were measured less frequently (for example alkyl nitrates and particulate nitrate) are omitted from the sum of individual species to maintain a large data set for comparison. Since PANs, which are the sum of the 3 PAN-type compounds above, were measured every 2 s, a maximum of 31 h of coincident 1-s measurements are possible during the 62 h of flight on these 10 days. Figure 3 has 67,576 coincident 1-s measurements (19 h), with in-flight instrument calibrations, zero determinations, diagnostics, and malfunctions that account for the remaining time.

[14] A bivariate linear least squares fit of (NO + NO_2 + HNO_3 + PANs) to NO_y, weighted by measurement imprecision, has a slope of 0.985, an intercept of negative 0.16 ppbv, and a high correlation coefficient (r = 0.99). The difference from a slope of one and intercept of zero is not significant, since it is far less than the instrumental uncertainties (Table 1). Uncertainty in the sum of the reactive nitrogen compounds varies with partitioning and concentration, but for a commonly observed aged plume with 5 ppbv HNO_3 and 2 ppbv NO_2 and PANs (e.g., Figure 2a, transect 4), the uncertainty in the sum of the individual species is 11% and the uncertainty in NO_y is 14%. Because the highest values of NO_y occurred in concentrated fresh plumes where NO_x dominated, the NO_x and NO_y measurements largely determine the slope of the linear fit. A more rigorous test of measurement accuracy for reactive nitrogen reservoir species compares the sum of measured HNO_3 and PANs to the measured difference between NO_y and NO_x (Figure 4). The bivariate linear least squares fit of HNO_3 + PANs to $NO_y - NO_x$ has a slope of 0.94, an intercept of negative 0.05 ppbv, and a high correlation coefficient (r = 0.97), demonstrating that nearly 100% of the NO_x oxidation products are accounted for by HNO_3 and PANs. The sum of eight alkyl nitrates measured in canisters during the flights was 2% of $NO_y - NO_x$ on average and accounts for some of the difference between HNO_3 + PANs and $NO_y - NO_x$. Similar to the findings from an earlier aircraft study in the Houston area in 2000 [*Neuman et al.*, 2002; *Ryerson et al.*, 2003], only a few percent of the measured NO_y is unaccounted for on average, but 10–15% measurement uncertainty in the sum of reactive nitrogen species remains.

[15] Other infrequently or unmeasured reactive nitrogen species were present in the atmosphere, but they were not abundant in the majority of the measurements reported here. The absolute difference between HNO_3 + PANs and $NO_y - NO_x$ is less than 1 ppbv in more than 93% of the measurements.

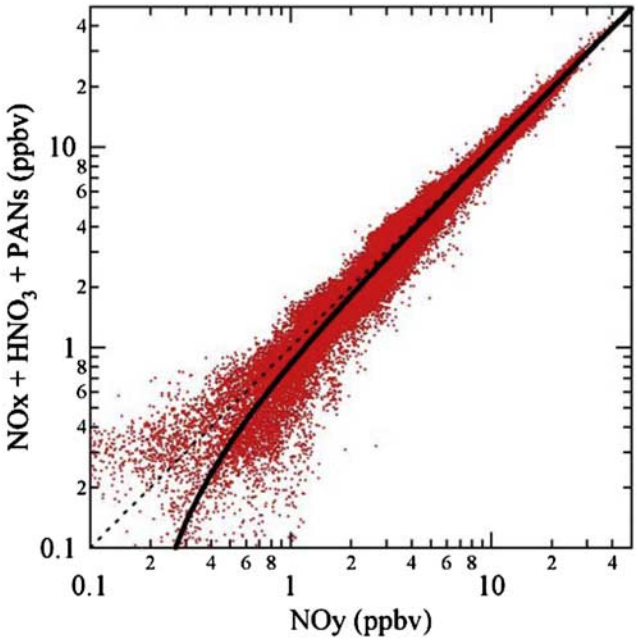

Figure 3. Measurements of the sum of individually measured reactive nitrogen compounds versus the measured NO_y for the 10 daytime flights in the Houston area. Each red dot represents a 1-s measurement. The dashed line is a one-to-one line, and the solid line is a linear least squares fit to the data, with a slope of 0.985 and r = 0.99.

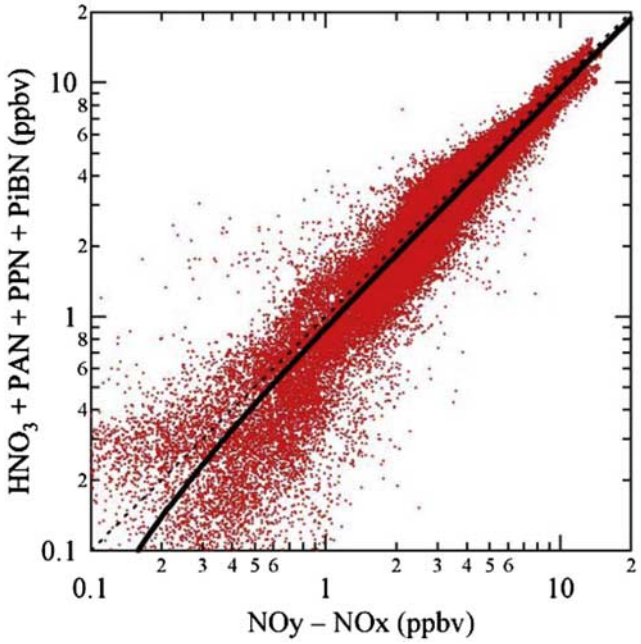

Figure 4. Same as Figure 3 but for the sum of individually measured reactive nitrogen reservoir species versus the difference between NO_y and NO_x. The solid line is a linear least squares fit to the data, with a slope of 0.94 and r = 0.97.

The largest differences are in isolated plumes from petrochemical industrial sources along the Houston ship channel, where $NO_y - NO_x$ often exceeds HNO_3 + PANs by 1–3 ppbv. In these plumes, rapid NO_x oxidation and O_3 formation occurs, and unmeasured alkyl nitrates [*Rosen et al.*, 2004] may be formed.

3.3. Reactive Nitrogen Partitioning

[16] The partitioning of NO_y between its constituents helps identify physical and chemical processes that occur in a plume. In the farthest downwind plume transects, NO_x was highly oxidized and accounted for only 10% to 20% of NO_y, and the partitioning of NO_x oxidation products between HNO_3 and PANs varied considerably. The HNO_3 and PANs produced in plumes exceeded background mixing ratios measured upwind of Houston. Background values were HNO_3 < 1 ppbv and PANs < 0.7 ppbv, except on 27 September when recirculated continental air had 3 ppbv HNO_3 and 1 ppbv PANs. In the center of plumes transported 50–170 km from Houston, HNO_3 ranged from 4 to 11 ppbv and PANs were 2–6 ppbv on 9 of the 10 flights. The exception occurred on 21 September 2006, when wind speeds were 10 m/s, and HNO_3 never exceeded 2 ppbv and PANs were less than 1.5 ppbv. In aged plumes far downwind from the Houston urban area, HNO_3 mixing ratios were their largest and usually constituted the majority of NO_y. In contrast, the largest PANs mixing ratios were in isolated plumes near the Houston ship channel. These PANs formed rapidly in plumes that had been transported less than 2 h, and were as high as 5.9 ppbv and sometimes exceeded HNO_3.

3.4. Emission Ratios

[17] Chemical transformation processes are examined by comparing enhancement ratios of pollutants in downwind transects to those near the source of emissions. An enhancement ratio for two pollutants in a plume is the quotient of the above-background mixing ratios for the two compounds. CO and NO_x were often coemitted, and the CO to NO_y enhancement ratio ($\Delta CO/\Delta NO_y$, where the Δ represents the contribution from Houston sources above the background) would remain constant during plume transport in the absence of downwind chemical production (e.g., CO production) or depositional loss (e.g., HNO_3 loss). For example, $\Delta CO/\Delta NO_y$ remained constant in plumes from urban areas on the U.S. east coast that were transported hundreds of kilometers over the North Atlantic Ocean, where transport occurred above the marine boundary layer such that depositional losses were low [*Neuman et al.*, 2006]. Close-in plume transects that captured emissions from both the urban area and ship channel industries and were within 20 km of the center of the urban area are used to determine CO to NO_y emission ratios from the urban and petrochemical sources. In these fresh plumes, nearly all NO_y enhancements were from NO_x, such that $\Delta CO/\Delta NO_x$ is nearly equal to $\Delta CO/\Delta NO_y$. NO_y is used here to account for small NO_x oxidation that may have occurred and for use in comparisons with transects farther downwind when NO_x was highly oxidized.

[18] Emissions of CO and NO_x from industries located near the Houston ship channel came from many different point sources located in close proximity and the relative CO and NO_x emissions from each source differed substantially. Consequently, CO and NO_x are not highly correlated in these close-in transects of ship channel emissions. Downwind, the emissions from many point sources coalesce, so that CO and NO_y are correlated (Figure 2), and slopes of bivariate linear least squares regressions can be used as a measure of the enhancement ratio. Emission ratios in fresh plumes, where CO and NO_y were less well-correlated, are determined instead by integrating background-subtracted mixing ratios across a plume, where background CO and NO_y are determined from measurements upwind. Observed $\Delta CO/\Delta NO_y$ are shown in Figure 5 as a function of time of day for 18 close-in transects. The CO to NO_y emission ratio

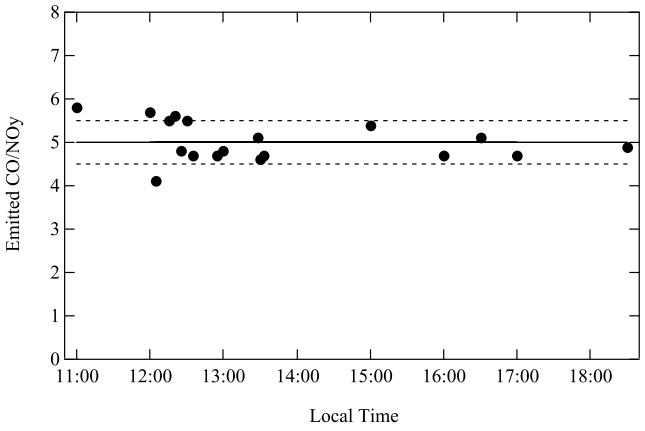

Figure 5. Measured CO to NO_y enhancement ratios in crosswind plume transects of fresh emissions from the Houston area, averaging over both the urban and ship channel source regions. The solid line is the average value, and the dashed lines represent 1 standard deviation from the average.

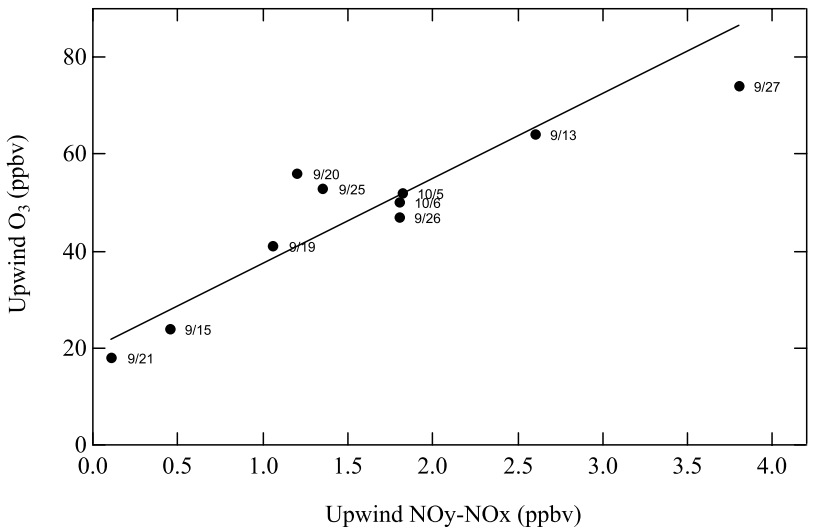

Figure 6. Background O_3 and $NO_y - NO_x$ mixing ratios averaged over transects upwind of Houston on each daytime flight. The line has a slope of 18.

during the study averaged 5.0 ± 0.5 and did not depend on the time of emission for observations from 1100 to 1800 local time.

[19] Plume transects were performed farther downwind during the afternoon when wind speeds were moderate (5.6 ± 2.3 m/s) and plumes were transported up to several hours after emission. Hence, most of the measured pollutants were emitted during the late morning or early afternoon, with approximately half emitted between 1100 and 1300 and over 90% emitted between 0800 and 1500. Limitations on flight duration necessitated that the aircraft conduct successive downwind transects more rapidly than the air was advected the same distance. As a result, the plume studies were not Lagrangian, but instead captured a spectrum of emission times. The farthest downwind transects sampled the earliest emissions and may include some contributions from nighttime emissions. During night in the Houston area, wind speeds and boundary layer depth were low, and pollutants were often concentrated with CO > 1 ppmv and NO_x > 100 ppbv. Nighttime CO to NO_x ratios measured at four different Continuous Ambient Monitoring Stations in the Houston urban area maintained by the Texas Council on Environmental Quality (TCEQ) and the City of Houston were approximately 8 during September 2006 (http://www.tceq.texas.gov/compliance/monitoring/air/monops/hourly_data.html). The WP-3 aircraft also flew into the nighttime boundary layer on 12 October 2006, when fresh emissions were sampled and $\Delta CO/\Delta NO_y$ was measured to range from 8 to 10. Measurements of motor vehicle emissions in Houston show that the contribution from diesel exhaust (with low CO/NO_x compared to gasoline) is less during the late afternoon compared to earlier in the day [*McGaughey et al.*, 2004], and hence may cause emission ratios to vary diurnally. If late afternoon emissions are trapped in a shrinking nighttime boundary layer, nighttime CO to NO_y ratios in the urban area may be larger than daytime ratios.

4. Analysis

[20] The enhancement ratios of trace gases measured in plumes are used to assess transformations that occur during transport. Here the ratios are determined several ways to reduce the effects of artifacts of a particular analysis technique. Two different types of least squares regressions are performed and compared to results derived from integrating mixing ratios across plumes. Enhancement ratios are derived from slopes of linear fits to pairs of 1-s data using least squares regression that allow uncertainty in both variables. Every measurement is weighted by $1/\sigma^2$, where σ is the measurement imprecision indicated in Table 1. These ratios are identified here as weighted bivariate fits. Ratios are also determined from correlation slopes obtained from standard one-sided linear least squares regressions of only the dependent variable, without weighting the data. Last, enhancement ratios are determined by integrating background-subtracted mixing ratios across plumes, as described in section 3.4. Each method is subject to different biases and uncertainties. The uncertainty in curve fitting is larger when the sources and sinks differ for the two compounds such that their covariation is diminished. Using plume integrations to attribute changes in enhancement ratios to production and loss of the measured compounds assumes that the primary or precursor emissions are unchanging, the background is constant and known, and both species are similarly vertically distributed in the boundary layer [*Trainer et al.*, 1995]. Some of these assumptions and approximations are examined in the following analysis.

4.1. Background Mixing Ratios

[21] The background levels of pollutants varied considerably according to the history of the air masses upwind of Houston (section 2.2) and affected the measured relationships between pollutants in plumes. With constant background levels over the course of a plume study, correlation slopes from linear least squares regressions accurately represent enhancement ratios of pollutants from local sources, since dilution of inert gases with a constant background does not alter the species' relationships [*McKeen et al.*, 1996]. With background levels that change across a plume transect, however, correlation slopes represent a combination of enhancement ratios from local sources and the background air. If the background pollutants have varying concentrations with different enhancement ratios but comparable

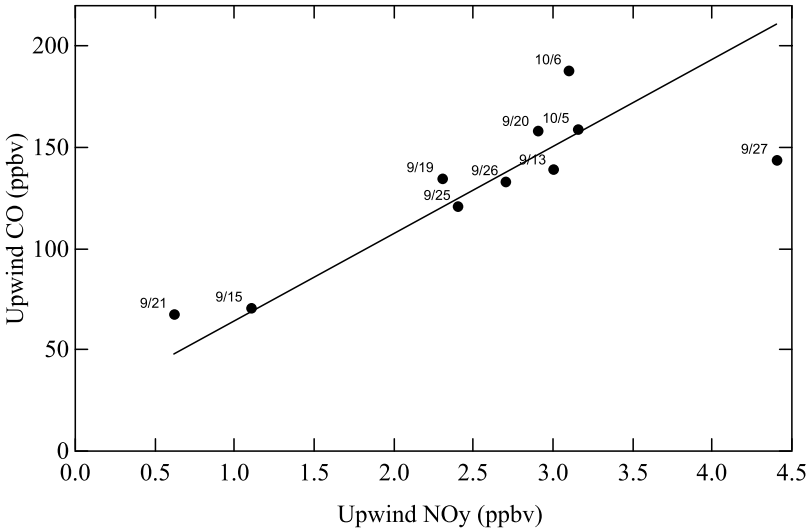

Figure 7. The same as Figure 6 but for CO and NO_y. The line has a slope of 40.

magnitudes to the plume mixing ratios, then correlation slopes do not accurately represent emissions or processing from the local source alone. Similarly, enhancement ratios of pollutants determined from plume integrations where background variability cannot be quantified and accurately subtracted do not represent solely the contributions from a local source.

[22] The average upwind CO, NO_y, O_3, and $NO_y - NO_x$ mixing ratios on the ten daytime flights are shown in Figures 6 and 7. The background O_3 levels and their association with wind direction are consistent with surface measurements in the Houston area during the summer of 2006 [*Rappenglück et al.*, 2008]. Assuming that the background air is a mixture of clean Gulf air and polluted continental air, as is suggested by the nearly linear relationships in Figures 6 and 7, then enhancement ratios for the background air can be derived from linear fits to the average upwind background mixing ratios measured on each flight. Background air masses had $\Delta CO/\Delta NO_y = 40$ (Figure 7) and $\Delta O_3/\Delta(NO_y - NO_x) = 18$ (Figure 6). In the absence of local sources, the mixing of clean and polluted background air alone yields $\Delta CO/\Delta NO_y$ approximately a factor of 8 higher than both Houston emission ratios and emission ratios from other urban areas [*Parrish et al.*, 2002], and over a factor of 4 higher than assumed nighttime ratios. The large $\Delta CO/\Delta NO_y$ in the background air is clearly affected by sources other than fresh local emissions.

[23] Variable mixing of clean air with aged polluted air can change background levels across a plume transect and influence observed enhancement ratios. As an example, Figure 8 shows 1-s measurements of CO, NO_y, O_3, and $NO_y - NO_x$ mixing ratios in the farthest downwind plume transect (Figure 1) on 15 September 2006. The aircraft flew from NE to SW, and the winds were from the SE at 5 m/s. North of Houston (~1455 local time (LT)), the background air was influenced by polluted continental air, while west of Houston (~1515 LT) the background air was more influenced by cleaner air from the Gulf of Mexico. The enhancements in CO (~50 ppbv) and O_3 (~20 ppbv) from the local Houston source are similar in magnitude to the changes in the background. Using the measurements obtained on both sides of the Houston plume, the background air has enhancement ratios of $\Delta CO/\Delta NO_y = 40$ and $\Delta O_3/\Delta(NO_y - NO_x) = 19$. Consequently, the correlation slopes obtained from weighted bivariate fits to this plume data ($\Delta CO/\Delta NO_y = 13$ and $\Delta O_3/\Delta(NO_y - NO_x) = 9$) are elevated in part owing to the variability in the background mixing ratios. Further, plume dilution decreases enhancements from local sources relative to background mixing ratios, so that the influence of variable background levels on measured enhancement ratios increases as plumes are transported.

[24] If background values are known at all times, the measurements can be corrected to isolate the influence of local sources above the background. However, changing backgrounds were most prominent here when wind speeds were high and variable, causing the mixing of background air with the Houston plume to vary in time and location during plume transport. This temporal and spatial variability in the background mixing ratios increases the uncertainty in extracting local contributions from the measurements. As a result, when local sources emitted into a large and variable background, plume processes were obscured. Thus,

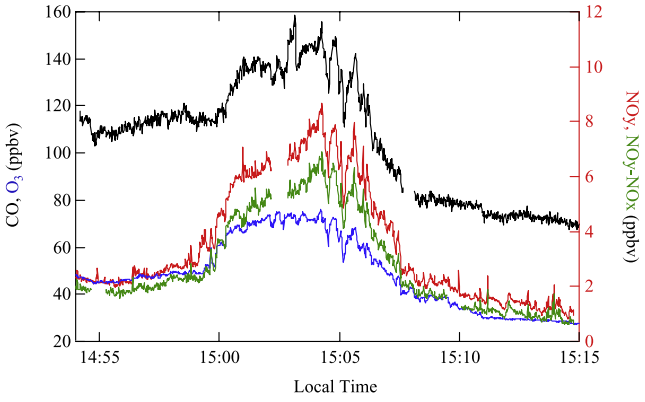

Figure 8. One-second measurements of O_3 (blue), CO (black), NO_y (red), and $NO_y - NO_x$ (green) from a plume transect 70 km downwind from Houston on 15 September 2006.

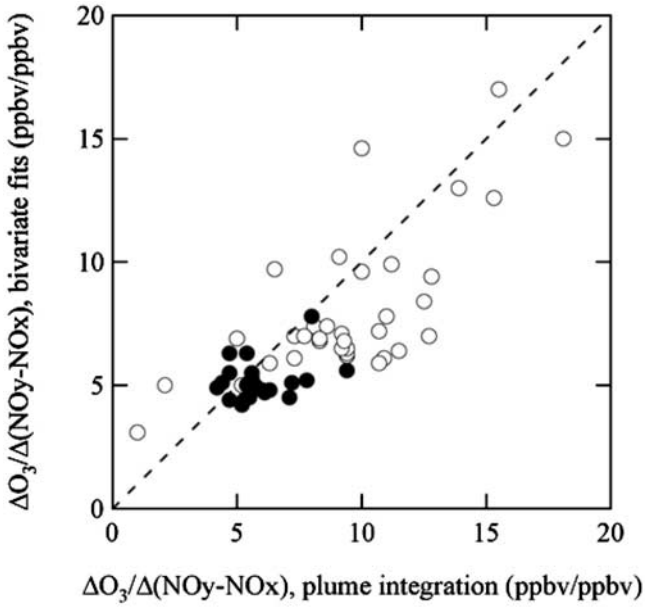

Figure 9. Comparison of $\Delta O_3/\Delta(NO_y - NO_x)$ enhancement ratios determined by weighted bivariate fits and plume integration. The solid circles are from plume transects with constant backgrounds on 20, 25, and 26 September and 5 October 2006, and the open circles are from the other six flights when backgrounds were variable. The dashed line has a slope of 1 and intercept of 0.

enhancement ratios are interpreted to represent emission ratios and OPEs only on days when measured CO upwind was equivalent (within 10 ppbv) to that outside of plumes in downwind transects. On 20, 25, and 26 September and 5 October, background mixing ratios were nearly constant, and on 13, 15, 19, 21, and 27 September and 6 October, background mixing ratios varied in location and time.

4.2. Relationship of Ozone to NO_x Oxidation Products

[25] The processes responsible for the relationship between O_3 and reactive nitrogen in coalesced urban and industrial plumes downwind from Houston are identified here. In aged plumes, O_3 was strongly correlated with the products of NO_x oxidation. NO_x oxidation products are determined here from the difference $NO_y - NO_x$, although they could be determined similarly from the sum HNO_3 + PANs (section 3.2). In aged plumes, O_3 enhancements (typically many tens of ppbv) were much greater than NO_2 enhancements (typically a few ppbv). Since NO_2 was only a few percent of O_3, there is little difference between representing O_3 formation by either O_3 or $O_3 + NO_2$, which is sometimes used to include additional O_3 formation that will occur once NO_2 is photolyzed. In the following discussion, O_3 formation is quantified by enhancements in O_3 alone.

[26] $\Delta O_3/\Delta(NO_y - NO_x)$ determined from weighted bivariate fits is similar to that determined using integrals of background-subtracted mixing ratios across a plume. The comparison of the two methods for 65 crosswind plume transects is shown in Figure 9. On average, $\Delta O_3/\Delta(NO_y - NO_x)$ determined by bivariate fits is 12% smaller than from plume integration, and the 2 methods never differ by more than 50%. Standard single-sided linear regression (not shown) yields smaller $\Delta O_3/\Delta(NO_y - NO_x)$ that are on average half that determined by plume integration. These smaller slopes reflect the relatively poor correlation between $\Delta O_3/\Delta(NO_y - NO_x)$, found especially in younger plumes. The weighted bivariate fits provide a more reliable fit to the data here, as demonstrated by the good agreement with the plume integration approach.

[27] The relationship between O_3 and NO_x oxidation products in coalesced plumes from Houston urban and industrial sources is similar in all downwind plume transects on the four flights when background mixing ratios were constant. As an example, Figure 10 shows 1-s measurements of O_3 versus $NO_y - NO_x$ for the four downwind plume transects on 25 September 2006 (time series shown in Figure 2). $\Delta O_3/\Delta(NO_y - NO_x)$ in each plume transect, determined by plume integration and weighted bivariate fits, ranges from 5.2 to 6.7. The blue line determined from a weighted bivariate fit to data from transect 4 (50 km and 2 h downwind, Figures 1 and 2) has a slope of 5.8 and r = 0.84. In the 24 plume transects performed when background mixing ratios were constant on 20, 25, and 26 September and 5 October, $\Delta O_3/\Delta(NO_y - NO_x)$ is 5.9 ± 1.2 and is independent of downwind distance. Changing backgrounds on 13, 15, 19, 21, and 27 September and 6 October cause determinations of $\Delta O_3/\Delta(NO_y - NO_x)$ to average nearly a factor of 2 higher and increase with downwind distance, reflecting the importance of variable mixing of polluted air with transported plumes to this observed ratio.

4.3. Relationship of Carbon Monoxide to Reactive Nitrogen

[28] Observed $\Delta CO/\Delta NO_y$ varies similarly to $\Delta O_3/\Delta(NO_y - NO_x)$, and this similarity elucidates the cause for the dependence of $\Delta O_3/\Delta(NO_y - NO_x)$ on flight date and downwind distance. $\Delta CO/\Delta NO_y$ is calculated here using both linear least squares regression and plume integration. Standard single sided linear least squares regressions yield $\Delta CO/\Delta NO_y$ approximately one third smaller than those determined by weighted bivariate fits or plume integration. $\Delta CO/\Delta NO_y$ from weighted bivariate fits agree

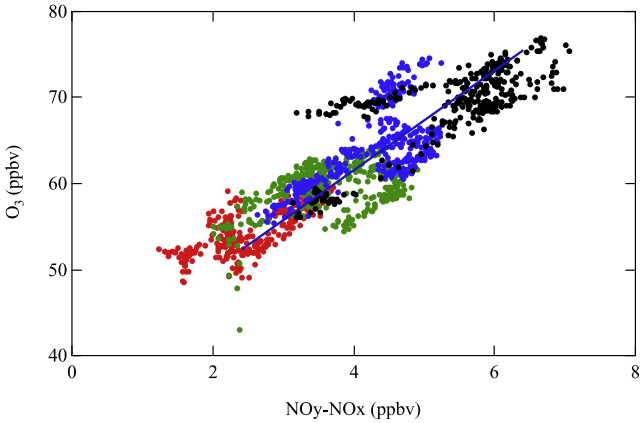

Figure 10. One-second measurements of O_3 versus $NO_y - NO_x$ for four plume transects downwind from Houston on 25 September 2006. The red circles are from transect 2 shown in Figures 1 and 2, the green are from transect 3, the blue are from transect 4, and the black are from transect 5. The blue line is from a linear fit to the data in transect 4.

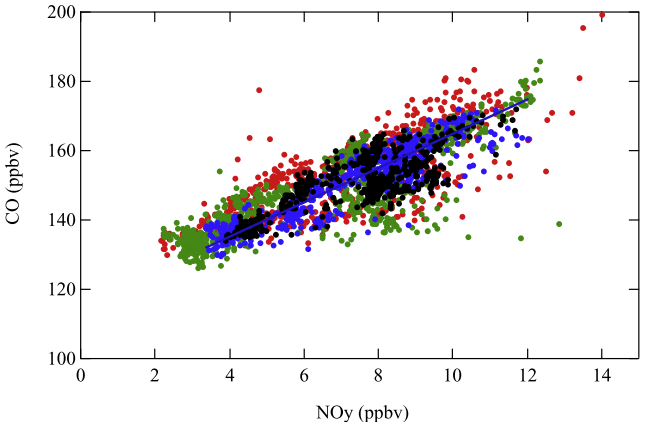

Figure 11. The same as Figure 10 but for CO and NO_y.

with values from plume integration to within 3%, over a range of values that vary over a factor of 3. This agreement reflects the improved accuracy obtained by using bivariate fits over single-sided fits when the measured species are not perfectly correlated. The relationship between CO and NO_y is shown in Figure 11 for the four downwind plume transects on 25 September (transects 2–5, Figures 1 and 2). The blue line, which is from a weighted bivariate fit of data from transect 4, has a slope of 4.9 and r = 0.91. For the 24 plume transects conducted on the 4 days with constant background mixing ratios, $\Delta CO/\Delta NO_y$ averages 5.7 ± 1.1, which is nearly equivalent to the value at emission (Figure 5). On the other six flights, changing backgrounds cause $\Delta CO/\Delta NO_y$ to vary with values often over a factor of 2 larger than emission ratios. $\Delta CO/\Delta NO_y$ varies with flight date and downwind distance similarly to $\Delta O_3/\Delta(NO_y - NO_x)$ since both enhancement ratios are elevated when transported plumes mix with aged pollution.

5. Discussion

[29] Variable mixing of polluted background air with plumes can limit the utility of observed enhancement ratios for quantifying plume processes. The causes for the changing backgrounds observed here and the limits they impose on data interpretation are examined in this section.

5.1. HNO_3 Loss

[30] The air measured upwind of Houston was often highly polluted compared to clean air from marine regions (Figures 6 and 7) with large enhancements in CO relative to NO_y and O_3 relative to $NO_y - NO_x$ (section 4.1). Here additional measurements are investigated to examine the possibility that HNO_3 removal affected the background enhancement ratios.

[31] Data from coincident particle measurements are used to assess the possibility that gas to particle conversion affected gas phase HNO_3 concentrations. Aircraft measurements of particulate nitrate by an aerosol mass spectrometer (R. Bahreini et al., Organic aerosol formation in urban and industrial plumes near Houston and Dallas, Texas, submitted to *Journal of Geophysical Research*, 2009) demonstrate that fine particulate nitrate (diameter less than 1 μm) was a very small fraction (typically about 2%) of total nitrate (particulate nitrate + HNO_3) in the Houston plume transects. The agreement between $NO_y - NO_x$ and HNO_3 + PANs (Figure 4) further indicates a small contribution of aerosol nitrate to NO_y, since fine particulate nitrate detected by an NO_y instrument [*Miyazaki et al.*, 2005] would cause $NO_y - NO_x$ to exceed HNO_3 + PANs. Ammonia, which can associate with HNO_3 to form fine particulate nitrate, was measured to be low (90% of the measurements were less than 3 ppbv) except in a few concentrated ammonia plumes from point sources (<1% of the measurements were > 5 ppbv (J. B. Nowak et al., manuscript in preparation, 2009)). Additionally, during these summer and fall daytime flights, high temperatures resulted in large ammonium nitrate dissociation constants, so that the partitioning of nitrate between the gas and particle phases favors gas phase HNO_3 over particulate ammonium nitrate. HNO_3 also can be lost to coarse particles. Aerosol sizing instruments determined particle size distributions for particles with physical diameters up to 8.3 μm. The measured coarse particle volume was not large enough to account for HNO_3 loss that could substantially elevate $\Delta CO/\Delta NO_y$. HNO_3 loss to particles is not evident here and does not explain the depletion of NO_y relative to CO measured in background air in the upwind transects.

[32] HNO_3 can be removed from the atmosphere by wet and dry deposition. Clouds were present at the top of the boundary layer on several days, but no precipitation events occurred along the plume trajectories during the 10 flights studied here. Additionally, no precipitation was reported in the Houston area in late September or early October 2006, but mid-September had several days with rain. Thus, air masses sampled upwind from Houston on the earlier flights may have been affected by precipitation that could reduce NO_y relative to CO in the background air. In this study with boundary layer depths typically 1.5 km, HNO_3 lifetimes to dry deposition are calculated to be approximately 14 h for the few cm/s deposition velocities reported for grasslands and forests [*Huebert and Robert*, 1985; *Hanson and Lindberg*, 1991]. This rapid depositional loss, compared to CO and O_3, may also explain the large $\Delta CO/\Delta NO_y$ and $\Delta O_3/\Delta(NO_y - NO_x)$ in aged polluted background air.

[33] In the absence of HNO_3 loss to particles or wet deposition during plume transport, $\Delta CO/\Delta NO_y$ is expected to remain nearly constant in plumes emitted into constant backgrounds and transported only a few hours. Dry deposition of HNO_3 during a few hours of plume transport should be small given the 14-h lifetime calculated above, and CO, which has a lifetime of several weeks, is conserved on the time scales of hours. Although CO production from VOC oxidation will increase CO mixing ratios [*Chin et al.*, 1994], this apparently did not substantially alter the CO mixing ratios here. The total outflow of CO from the Houston area measured in each plume (see *Trainer et al.* [1995] for the method employed here to determine this flux) did not increase downwind on the four flights with constant backgrounds. $\Delta CO/\Delta NO_y$ remained nearly constant in the plume transects on the four flights with constant backgrounds, consistent with previous work [*Ryerson et al.*, 2003] and with HNO_3 and CO lifetimes that are larger than plume transport times. HNO_3 deposition velocities were observed to vary widely in power plant plumes in Texas [*Neuman et al.*, 2004], and the

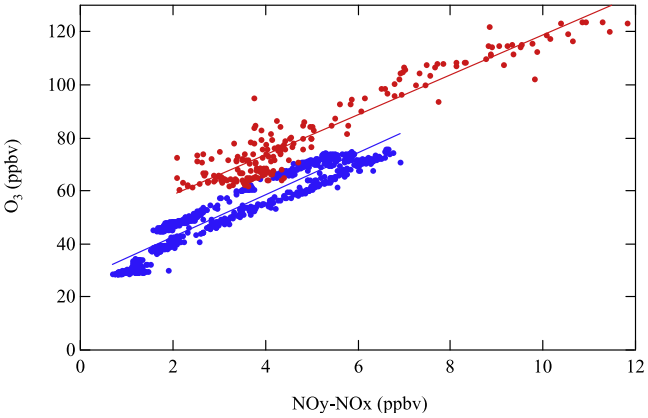

Figure 12. One-second measurements of O_3 versus $NO_y - NO_x$ for a transect of an isolated plume downwind from the Houston ship channel on 6 October (red circles) and from the transect 70 km downwind from Houston on 15 September (blue circles) shown in Figure 8. The lines are from weighted bivariate fits to the data.

results here are consistent with the lower values reported in that work.

5.2. Ozone Production Efficiency

[34] The sensitivity of O_3 production to NO_x emission has revealed the benefits that can be anticipated from NO_x reduction [*Ryerson et al.*, 2001], but such conclusions can only be reached if observationally based determinations of OPE are not affected by processes that degrade their representation of plume photochemistry. A wide range of $\Delta O_3/\Delta(NO_y - NO_x)$ values are observed in plume transects downwind from Houston urban and industrial sources under differing meteorological conditions (Figure 9), but OPE cannot always be derived accurately from the observed $\Delta O_3/\Delta(NO_y - NO_x)$. When background mixing ratios remain constant and loss of reactive nitrogen is low, the enhancements in primary and secondary pollutants caused by emissions from the Houston area can be quantified, and $\Delta O_3/\Delta(NO_y - NO_x)$ can be accurately interpreted as the OPE (section 4.2). When plumes mixed with changing backgrounds causing coincident increases in $\Delta CO/\Delta NO_y$ and $\Delta O_3/\Delta(NO_y - NO_x)$, the effects of photochemical production from local emissions cannot be separated from background variability, and the observed relationship between O_3 and $NO_y - NO_x$ cannot be interpreted as an OPE representative of plume photochemistry.

[35] The importance of carefully linking $\Delta O_3/\Delta(NO_y - NO_x)$ to OPE is illustrated in Figure 12 by comparing an aged coalesced plume to a concentrated plume from the Houston ship channel. The blue circles were measured 70 km from Houston on the farthest downwind transect on 15 September (Figure 8), and the red circles were measured 10–15 km downwind from the Houston ship channel on 6 October. In both plumes, O_3 and $NO_y - NO_x$ are highly correlated, and the observed $\Delta O_3/\Delta(NO_y - NO_x)$ from weighted bivariate fits are approximately 9. Despite the similarity in $\Delta O_3/\Delta(NO_y - NO_x)$, the high enhancement ratios in these two plumes do not indicate similar photochemistry.

[36] Changing background mixing ratios that include contributions from aged pollution depleted in NO_y and $NO_y - NO_x$ on 15 September elevate $\Delta CO/\Delta NO_y(=13)$ and $\Delta O_3/\Delta(NO_y - NO_x)$ in this plume. In the plume, the majority of the NO_y reservoir was HNO_3 (4 ppbv), with a smaller contribution from PANs (2 ppbv). When changes in background mixing ratios are comparable to enhancements from a local source in a transported plume (as on 15 September), regional changes in relationships between pollutants obscure and alter the signatures from the local source, and enhancement ratios do not represent the effects of local emissions alone. The 6 October plume in Figure 12 was from a geographically smaller source, such that the backgrounds were nearly constant on either side of this concentrated plume. In this plume, both O_3 and PANs had been formed in large abundance, and immediately downwind from the petrochemical industrial facilities located along the Houston ship channel. PANs (6 ppbv) were more abundant than HNO_3 (4 ppbv), and $\Delta CO/\Delta NO_y$ was 3. The relatively large enhancements in PANs compared to HNO_3 indicate the importance of VOC to the O_3 photochemistry in this plume. Since the backgrounds were constant and reactive nitrogen loss was low (as evidenced by $\Delta CO/\Delta NO_y$ equivalent to the value at emission), $\Delta O_3/\Delta(NO_y - NO_x)$ can be interpreted as the OPE. The OPE of 9 in this ship channel plume is higher than that measured in coalesced plumes as a consequence of rapid and efficient photochemistry. This finding is consistent with work that showed rapid and efficient O_3 formation in plumes from petrochemical industrial sources with large NO_x and reactive alkene emissions [*Ryerson et al.*, 2003]. Distinguishing these high OPE plumes from those that are affected by changing background pollution is facilitated by quantifying $\Delta CO/\Delta NO_y$ and background pollution levels upwind and adjacent to transported plumes.

6. Conclusions

[37] Ozone production efficiency (OPE), which is the integrated number of O_3 molecules formed for each NO_x molecule oxidized, is determined from the observed $\Delta O_3/\Delta(NO_y - NO_x)$ enhancement ratios measured in plumes downwind from Houston urban and industrial areas. However, this ratio can be strongly affected by the background pollution. On six daytime flights in the Houston area, transport and mixing was complicated, and polluted background air mixed with the plumes at different locations and times and caused changing backgrounds. $\Delta CO/\Delta NO_y$ and $\Delta O_3/\Delta(NO_y - NO_x)$ increase with downwind distance on these days. Elevated $\Delta CO/\Delta NO_y$ in aged polluted background air suggests that HNO_3 depositional loss had reduced the background NO_y abundance. On these 6 days when backgrounds changed and $\Delta CO/\Delta NO_y$ increases downwind, $\Delta O_3/\Delta(NO_y - NO_x)$ also increases downwind and is highly elevated and variable. Changing background levels affect the enhancement ratios so that OPE cannot be determined unambiguously from observed mixing ratios on these days. On the 4 days when background mixing ratios and $\Delta CO/\Delta NO_y$ are constant, the enhancement ratio of O_3 to $NO_y - NO_x$ averages 5.9 ± 1.2 and is interpreted as representing the OPE. Higher OPE is observed in plumes dominated by Houston ship channel emissions, where O_3

and PANs are formed rapidly. The OPEs determined here are consistent with previous results from the same region. Using data from the Texas 2000 study, the ratio of O_3 to NO_x oxidation products in plumes heavily influenced by the Houston ship channel were 11 to 12, and the O_3 yield was about a factor of two smaller in isolated Houston urban plumes [*Ryerson et al.*, 2003; *Daum et al.*, 2003].

[38] Literature reports of OPE span a wide range of values [e.g., *Trainer et al.*, 1993; *Hirsch et al.*, 1996; *Kasibhatla et al.*, 1998; *Berkowitz et al.*, 2004; *Griffin et al.*, 2004]. Using the relationship between accumulated O_3 and NO_x emissions, the large-scale regional OPE was estimated to range from 2 to 3 O_3 molecules per NO_x molecule in the eastern United States [*Kasibhatla et al.*, 1998]. In contrast, OPE in the eastern United States determined from observed linear regressions between O_3 and NO_x oxidation products have yielded OPEs several times higher and have been reported to increase with plume age [*Zaveri et al.*, 2003]. HNO_3 removal during plume transport has been suggested as the likely cause for the high OPE values estimated from such observations [*Trainer et al.*, 1993, 2000; *Kasibhatla et al.*, 1998]. The results shown here demonstrate that variable mixing of background air affected by HNO_3 removal with local pollution can also influence observationally based estimates of OPE. Background mixing ratios and $\Delta CO/\Delta NO_y$ provide indicators for distinguishing plumes with efficient O_3 formation from plumes with similarly high O_3 to NO_x oxidation products correlation slopes caused by variable mixing of aged polluted air depleted in HNO_3. Understanding the effects of transport and mixing on enhancement ratios of pollutants is critical for evaluating the significance of the wide range of values for OPE that appear in the literature (e.g., Table 1 of *Griffin et al.* [2004] shows results from 18 studies of ozone production).

[39] **Acknowledgments.** The Air Quality and the Climate Research and Modeling Programs of the National Oceanic and Atmospheric Administration (NOAA) and the Texas Commission on Environmental Quality (TCEQ) supported the WP-3 measurements. Much of the analysis was supported by TCEQ under grant 582-8-86246. J.A.N. thanks Charles Brock and Ann Middlebrook for helpful discussions and for providing measurements of particle size and composition.

References

Berkowitz, C. M., T. Jobson, G. Jiang, C. W. Spicer, and P. V. Doskey (2004), Chemical and meteorological characteristics associated with rapid increases of O_3 in Houston, Texas, *J. Geophys. Res.*, *109*, D10307, doi:10.1029/2003JD004141.

Chin, M., D. J. Jacob, J. M. Munger, D. D. Parrish, and B. G. Doddridge (1994), Relationship of ozone and carbon monoxide over North America, *J. Geophys. Res.*, *99*, 14,565–14,573, doi:10.1029/94JD00907.

Darby, L. S. (2005), Cluster analysis of surface winds in Houston, Texas, and the impact of wind patterns on ozone, *J. Appl. Meteorol.*, *44*, 1788–1806, doi:10.1175/JAM2320.1.

Daum, P. H., L. I. Kleinman, S. R. Springston, L. J. Nunnermacker, Y.-N. Lee, J. Weinstein-Lloyd, J. Zheng, and C. M. Berkowitz (2003), A comparative study of O_3 formation in the Houston urban and industrial plumes during the 2000 Texas Air Quality Study, *J. Geophys. Res.*, *108*(D23), 4715, doi:10.1029/2003JD003552.

Griffin, R. J., C. A. Johnson, R. W. Talbot, H. Mao, R. S. Russo, Y. Zhou, and B. C. Sive (2004), Quantification of ozone formation metrics at Thompson Farm during the New England Air Quality Study (NEAQS) 2002, *J. Geophys. Res.*, *109*, D24302, doi:10.1029/2004JD005344.

Hanson, P. J., and S. E. Lindberg (1991), Dry deposition of reactive nitrogen compounds: A review of leaf, canopy, and non-foliar measurements, *Atmos. Environ., Ser. A*, *25*, 1615–1634.

Hirsch, A. I., J. W. Munger, D. J. Jacob, L. W. Horowitz, and A. H. Goldstein (1996), Seasonal variation of the ozone production efficiency per unit NO_x at Harvard Forest, Massachusetts, *J. Geophys. Res.*, *101*, 12,659–12,666, doi:10.1029/96JD00557.

Huebert, B. J., and C. H. Robert (1985), The dry deposition of nitric acid to grass, *J. Geophys. Res.*, *90*, 2085–2090, doi:10.1029/JD090iD01p02085.

Kasibhatla, P., W. L. Chameides, R. D. Saylor, and D. Olerud (1998), Relationships between regional ozone pollution and emissions of nitrogen oxides in the eastern United States, *J. Geophys. Res.*, *103*, 22,663–22,669, doi:10.1029/98JD01639.

Kleinman, L. I., P. H. Daum, Y.-N. Lee, L. J. Nunnermacker, S. R. Springston, J. Weinstein-Lloyd, and J. Rudolph (2005), A comparative study of ozone production in five U.S. metropolitan areas, *J. Geophys. Res.*, *110*, D02301, doi:10.1029/2004JD005096.

Liu, S. C., M. Trainer, F. C. Fehsenfeld, D. D. Parrish, E. J. Williams, D. W. Fahey, G. Hubler, and P. C. Murphy (1987), Ozone production in the rural troposphere and the implications for regional and global ozone distributions, *J. Geophys. Res.*, *92*, 4191–4207, doi:10.1029/JD092iD04p04191.

McGaughey, G. R., N. R. Desai, D. T. Allen, R. L. Seila, W. A. Lonneman, M. P. Fraser, R. A. Harley, A. K. Pollack, J. M. Ivy, and J. H. Price (2004), Analysis of motor vehicle emissions in a Houston tunnel during the Texas Air Quality Study 2000, *Atmos. Environ.*, *38*, 3363–3372, doi:10.1016/j.atmosenv.2004.03.006.

McKeen, S. A., S. C. Liu, E.-Y. Hsie, X. Lin, J. D. Bradshaw, S. Smyth, G. L. Gregory, and D. R. Blake (1996), Hydrocarbon ratios during PEM-WEST A: A model perspective, *J. Geophys. Res.*, *101*, 2087–2109, doi:10.1029/95JD02733.

Miyazaki, Y., et al. (2005), Contribution of particulate nitrate to airborne measurements of total reactive nitrogen, *J. Geophys. Res.*, *110*, D15304, doi:10.1029/2004JD005502.

Munger, J. M., S. M. Fan, P. S. Bakwin, M. L. Goulden, A. H. Goldstein, A. S. Colman, and S. C. Wofsy (1998), Regional budgets for nitrogen oxides from continental sources: Variations of rates for oxidation and deposition with season and distance from source regions, *J. Geophys. Res.*, *103*, 8355–8368, doi:10.1029/98JD00168.

Neuman, J. A., et al. (2002), Fast-response airborne in situ measurements of HNO_3 during the Texas air Quality Study, *J. Geophys. Res.*, *107*(D20), 4436, doi:10.1029/2001JD001437.

Neuman, J. A., D. D. Parrish, T. B. Ryerson, C. A. Brock, C. Wiedinmyer, G. J. Frost, J. S. Holloway, and F. C. Fehsenfeld (2004), Nitric acid loss rates measured in power plant plumes, *J. Geophys. Res.*, *109*, D23304, doi:10.1029/2004JD005092.

Neuman, J. A., et al. (2006), Reactive nitrogen transport and photochemistry in urban plumes over the North Atlantic Ocean, *J. Geophys. Res.*, *111*, D23S54, doi:10.1029/2005JD007010.

Parrish, D. D., M. Trainer, D. Hereid, E. J. Williams, K. J. Olszyna, R. A. Harley, J. F. Meagher, and F. C. Fehsenfeld (2002), Decadal change in carbon monoxide to nitrogen oxide ratio in U.S. vehicular emissions, *J. Geophys. Res.*, *107*(D12), 4140, doi:10.1029/2001JD000720.

Rappenglück, B., R. Perna, S. Zhong, and G. A. Morris (2008), An analysis of the vertical structure of the atmosphere and the upper-level meteorology and their impact on surface ozone levels in Houston, Texas, *J. Geophys. Res.*, *113*, D17315, doi:10.1029/2007JD009745.

Rosen, R. S., E. C. Wood, P. J. Wooldridge, J. A. Thornton, D. A. Day, W. Kuster, E. J. Williams, B. T. Jobson, and R. C. Cohen (2004), Observations of total alkyl nitrates during Texas Air Quality Study 2000: Implications for O_3 and alkyl nitrate photochemistry, *J. Geophys. Res.*, *109*, D07303, doi:10.1029/2003JD004227.

Ryerson, T. B., et al. (2001), Observations of ozone formation in power plant plumes and implications for ozone control strategies, *Science*, *292*, 719–723, doi:10.1126/science.1058113.

Ryerson, T. B., et al. (2003), Effect of petrochemical industrial emissions of reactive alkenes and NO_x on tropospheric ozone formation in Houston, Texas, *J. Geophys. Res.*, *108*(D8), 4249, doi:10.1029/2002JD003070.

Sillman, S., D. He, M. R. Pippin, P. H. Daum, D. G. Imre, L. I. Kleinman, J. H. Lee, and J. Weinstein-Lloyd (1998), Model correlations for ozone, reactive nitrogen, and peroxides for Nashville in comparison with measurements: Implications for O_3-NO_x-hydrocarbon chemistry, *J. Geophys. Res.*, *103*, 22,629–22,644, doi:10.1029/98JD00349.

Trainer, M., et al. (1993), Correlation of ozone with NO_y in photochemically aged air, *J. Geophys. Res.*, *98*, 2917–2925, doi:10.1029/92JD01910.

Trainer, M., B. A. Ridley, M. P. Buhr, G. Kok, J. Walega, G. Hubler, D. D. Parrish, and F. C. Fehsenfeld (1995), Regional ozone and urban plumes in the southeastern United States: Birmingham, a case study, *J. Geophys. Res.*, *100*, 18,823–18,834, doi:10.1029/95JD01641.

Trainer, M., D. D. Parrish, P. D. Goldan, J. Roberts, and F. C. Fehsenfeld (2000), Review of observation-based analysis of the regional factors influencing ozone concentrations, *Atmos. Environ.*, *34*, 2045–2061, doi:10.1016/S1352-2310(99)00459-8.

Zaveri, R. A., C. M. Berkowitz, L. I. Kleinman, S. R. Springston, P. V. Doskey, W. A. Lonneman, and C. W. Spicer (2003), Ozone production

efficiency and NO_x depletion in an urban plume: Interpretation of field observations and implications for evaluating O_3-NO_x-VOC sensitivity, *J. Geophys. Res.*, *108*(D14), 4436, doi:10.1029/2002JD003144.

E. L. Atlas, Rosenstiel School of Marine and Atmospheric Sciences, University of Miami, 4600 Rickenbacker Causeway, Miami, FL 33149, USA.

R. Bahreini, F. C. Fehsenfeld, G. J. Frost, J. S. Holloway, J. A. Neuman, J. B. Nowak, J. Peischl, and A. G. Wollny, Cooperative Institute for Research in Environmental Sciences, University of Colorado at Boulder, UCB 216, Boulder, CO 80309, USA. (andy.neuman@noaa.gov)

F. Flocke and W. Zheng, Atmospheric Chemistry Division, National Center for Atmospheric Research, P.O. Box 3000, Boulder, CO 80305-3000, USA.

D. D. Parrish, T. B. Ryerson, and M. Trainer, Earth System Research Laboratory, NOAA, R/CSD 7, 325 Broadway, Boulder, CO 80305, USA.